ISSN 1070-3284, Russian Journal of Coordination Chemistry, 2023, Vol. 49, No. 7, pp. 437–445. © Pleiades Publishing, Ltd., 2023.
Russian Text © The Author(s), 2023, published in Koordinatsionnaya Khimiya, 2023, Vol. 49, No. 7, pp. 431–40.

Crystal Structure of Magnesium Comenate

L. I. Ivashchenko[a, *], S. V. Kozin[a, b], L. V. Vasil'eva[a], A. M. Vasil'ev[a], V. V. Dotsenko[a, c], N. A. Aksenov[c], and A. A. Kravtsov[a, b]

[a] *Kuban State University, Krasnodar, Russia*

[b] *Southern Scientific Center, Russian Academy of Sciences, Rostov-on-Don, Russia*

[c] *North-Caucasus Federal University, Stavropol, Russia*

**e-mail: levmag1@gmail.com*

Received October 2, 2022; revised December 13, 2022; accepted January 10, 2023

Abstract—The coordination compound $[Mg(HCom)_2(H_2O)_6]\cdot 2H_2O$ (**I**) was obtained by the reaction of comenic acid (H_2Com) with magnesium acetate in water. The formation of a new phase was confirmed by powder X-ray diffraction. The molecular formula of the compound was determined from energy dispersive X-ray fluorescence and thermogravimetry data. The thermo-oxidative stability of magnesium comenate was studied by simultaneous thermal analysis in air. The molecular structure of the complex was discussed on the basis of spectral data (NMR, IR, and UV spectroscopy) and studied in detail using X-ray diffraction (CCDC no. 2207835). Magnesium comenate crystallizes in the triclinic system, space group $P\bar{1}$, the structure is stabilized by intra- and intermolecular hydrogen bonds between the coordinated water molecules, acid anions, and $[Mg(H_2O)_6]^{2+}$.

Keywords: comenic acid, β-hydroxy-γ-pyrones, neuroprotective agents, magnesium complexes, X-ray diffraction

DOI: 10.1134/S1070328423600201

INTRODUCTION

Comenic acid (5-hydroxy-4-oxo-4*H*-pyran-2-carboxylic acid, H_2Com, H_2L) has long been actively used as a molecular platform for the preparation of new γ-pyrone (4-oxo-4*H*-pyran) derivatives and as complexing agent [1, 2]. The microbiological synthesis of H_2Com is based on bacterial processing of natural feedstock containing galactose with *Gluconobacter oxydans* [3].

Both comenic acid and its derivatives exhibit a number of biological effects. Comenic acid and its magnesium and lithium salts possess neuroprotective properties, showing pronounced antioxidant and moderate anxiolytic and antiamnestic behaviors [4–6].

The agent Baliz-2, containing comenic acid, was clinically proved to be effective in the treatment of gastrointestinal ulcer diseases and skin burns [7]. Comenic acid has an analgesic effect, functioning as a μ-opioid receptor agonist [8]. It was shown by theoretical calculations that the interaction with μ-opioid receptors is possible only in the case where H_2Com forms chelates with metal ions [9, 10]. Therefore, it is of interest to experimentally study the possibility of formation, structure, and properties of complex compounds of ligands of this type with Mg^{2+} ions in aqueous solution.

Magnesium agents are widely used and studied in pharmacology because of high biological activity of magnesium(II) salts. The Mg^{2+} ions have antihypertensive, antiarrhythmic, anti-inflammatory, and anticoagulant activities; hence, the use of magnesium agents may be useful for the prevention and treatment of cardiovascular diseases [11]. The Mg^{2+} ions can prevent the neuronal calcium overload by blocking the ion channels of NMDA receptors and control the function of γ-aminobutyric acid (GABA) inhibitory receptors [12]. Owing to these effects, magnesium(II) salts can be considered as potential means for the control of the post-stroke effects and treatment of neurodegenerative diseases of the CNS. A significant pharmacological problem is the search for new ligands that would synergistically enhance the effect of biometal ions. The established protective effect of H_2Com provides grounds for considering the acid as a potential ligand for Mg^{2+} ions in the context of the search for new neuroprotective and cardioprotective agents.

Previously, we studied the properties and biological effects of magnesium comenate [4, 13–15]; however, no data on the structural features of this compound are available from the literature. In this study, we report for the first time the results of structural and

spectral studies of magnesium comenate $[Mg(HCom)_2(H_2O)_6]\cdot 2H_2O$ (**I**).

EXPERIMENTAL

NMR spectra were measured on a JEOL 400 instrument (400 MHz for ^1H and 100 MHz for ^{13}C) in D_2O at 298 K. The residual solvent signals served as the standard. IR spectra were measured on a Bruker Vertex 70 FTIR spectrometer with an ATR attachment on a diamond crystal; the spectral resolution was ± 4 cm^{-1}. Elemental analysis was performed by the fundamental parameter method on an EDX-8000 energy dispersive X-ray analyzer. The product purity and the course of the reactions were monitored by TLC on Sorbfil PTSKh-AF-A plates (LLC Imid, Krasnodar) using an acetone–hexane mixture (1 : 1) as the eluent, iodine vapor for visualization, and UV detector. The starting compound used for the synthesis was $Mg(CH_3COO)_2\cdot 4H_2O$ (analytical grade, >99.5%, KhimKraft). All experiments were carried out using doubly distilled water.

Powder X-ray diffraction analysis was carried out on an XRD-7000 automated diffractometer (Shimadzu, Japan). The curves for the dependence of the diffraction intensity on the reflection angle 2θ were measured at room temperature (298 K). The measurement conditions were as follows: CuK_α radiation (1.54 Å), 40 kV, 30 mA, recording rate of 1° per min in the 2θ range of 10°–60° with a scanning step of 0.02; divergence slit (DS) of 1°; scattering slit (SS) of 1°; receiving slit (RS) of 0.3 mm; and exposure time of 1.2 s. The X-ray diffraction peaks were identified and quantitative phase content was determined using the PDWin 2.0 software package and the Crystallographica Search-Match package integrated into the hardware/software system of the instrument.

Thermogravimetric (TG) analysis was carried out on an STA-409 PC Luxx simultaneous thermal analyzer (Netzsch, Germany). The testing was performed in an oxidative atmosphere (air) in alundum crucibles under programmed isothermal heating with α-Al_2O_3 as the reference at a heating rate of 10°C/min in a temperature range of 30–1000°C.

Electronic absorption spectra were measured on a U-2900 double-beam spectrophotometer (Hitachi, Japan) in quartz cells (l = 10 mm) in the spectral range of 190–400 nm. The empirical spectra were smoothed by fast Fourier transform (FFT) using OriginLab 2019 software package.

5-Hydroxy-4-oxo-4*H*-pyran-2-carboxylic (comenic) acid was synthesized in 80% yield by glucose oxidation using 003 strain of the *Gluconobacter oxydans* bacteria according to reported procedures [16, 17] and purified by column chromatography.

IR (ν, cm^{-1}): 3339 (O^8–H(H_2L)), 3089 (C–H), 2997–2467 (O–H). ^1H NMR (D_2O; 298 K; δ, ppm): 7.03 (s, 1H, C^3–H), 8.02 (s, 1H, C^6–H). ^{13}C NMR (D_2O; 298 K; δ, ppm): 176.9 (C^4), 164.2 (COOH), 156.5 (C^2), 146.4 (C^5), 142.3 (C^6), 115.3 (C^3).

Magnesium 5-hydroxy-4-oxo-4*H*-pyran-2-carboxylate (comenate) (I) was synthesized using a modified procedure of [13] by treatment of a solution of comenic acid (1.00 g, 6.4 mmol) in water (25 mL) at a temperature of 80 ± 2°C with a solution of $Mg(CH_3COO)_2\cdot 4H_2O$ (0.69 g, 3.2 mmol) in water (5 mL). As a result, the reaction mixture acquired pH of 4.5–5.0 and a yellow color. Magnesium comenate was isolated from the solution by evaporation by ~3/4 of the initial volume after which it started to crystallize from the hot solution. The product was additionally recrystallized from doubly distilled water. The yield was 2.61 g (85%).

IR (ν, cm^{-1}): 3500 (O^8–H(H_2L)), 3190, 3093 (C–H), 2976 (O–H H_2O), 1691 ν(C^4=O), 1601 ν_{as}(COO^-), 1556 (C^1=O), 1462, 1352 ν_s(COO^-), 1271, 1213 (C^1–O), 1157 (C^5–O–H), 1101, 935, 893, 854, 804, 771, 663, 561, 517, 411.

^1H NMR (D_2O; 298 K; δ, ppm): 6.94 (s, 1H, C^3–H), 8.00 (s, 1H, C^6–H). ^{13}C NMR (D_2O; 298 K; δ, ppm): 177.2 (C^4), 165.3 (COOH), 158.6 (C^2), 146.1 (C^5), 142.0 (C^6), 114.4 (C^3).

For $C_{12}H_{22}O_{18}Mg$

Anal. calcd., %	C, 30.11	H, 4.63	O, 60.17	Mg, 5.08
Found, %	C, 28.11	H, 4.45	O, 57.81	Mg, 5.14

Single crystal X-ray diffraction study of **I** was carried out on a SuperNova automated four-circle diffractometer, Dual, Cu at zero, Atlas S2 (CuK_α, λ = 1.54184 Å) at 293(2) K. The structures were solved using the Olex2 [18] and SHELXT [19] program packages by the least-squares method. The remaining hydrogen atoms were located by direct methods using successive calculations of difference Fourier maps. The positions of atoms were refined by the full-matrix least-squares method on F^2_{hkl} in the anisotropic approximation for all non-hydrogen atoms with the SHELXL software [20]. The contributions of hydrogen atoms were taken into account in the calculations but not refined. In all cases, the positions of the highest peaks and the residual electron density values in the final Fourier difference maps were chemically insignificant.

The main X-ray diffraction experiment details and unit cell parameters were as follows: triclinic system, space group $P\bar{1}$, M = 478.60 g/mol, a = 6.7265(2), b = 7.0802(2), c = 10.7367(4) Å, α = 103.337(3)°, β = 96.095(2)°, γ = 103.071(2)°, V = 477.84(3) Å^3, Z = 1, μ(CuK_α) = 1.711 mm^{-1}, ρ(calcd.) = 1.663 g/cm^3, F(000) = 250.0; measurement angles θ = 8.584°–152.2°; ranges of reflection indices: $-8 \le h \le 8$, $-8 \le$

$k \le 8$, $-12 \le l \le 13$; 9635 measured reflections ($8.584° \le 2\theta \le 152.2°$); 1990 unique reflections (R_{int} = 0.0180, R_σ = 0.0104). R-factors ($I > 2\sigma(I)$): R_1 = 0.0248 (wR_2 = 0.0657), R-factors for all reflections: R_1 = 0.0251 (wR_2 = 0.0657); GOOF on F^2 1.107, $\Delta\rho_{max}/\Delta\rho_{min}$ = 0.38/–0.21 e Å^{-3}.

The atom coordinates and other parameters of the structures were deposited with the Cambridge Crystallographic Data Centre (CCDC no. 2207835; www.ccdc.cam.ac.uk/structures).

The elemental composition of the complex was determined by quantitative energy dispersive X-ray fluorescence spectroscopy using an EDX-8000 instrument (Shimadzu, Japan) based on a silicon drift detector (SDD) with a thermoelectric cooling. The analysis conditions were as follows: an X-ray tube with a rhodium anode was used as an excitation source; the exposure was 500 s; the diameter of the irradiated zone was 10 mm; the incidence angle on the sample was 45°, the scattering angle on the detector was 45°; and the radiation scattering and reflection processes took place in vacuum. The samples were prepared by grinding 1.0–1.2 g of the compound down to 10 μm size in an agate mortar. The suspension was pressed into pellets with a diameter of 20 mm (0.7 g of wax served as a substrate) using a 15 ton press mold.

RESULTS AND DISCUSSION

Magnesium comenate $[Mg(HCom)_2(H_2O)_6]\cdot 2H_2O$ (**I**) was prepared by the reaction of comenic acid with magnesium acetate hydrate on heating in water (Scheme 1). The structure of the reaction product was studied in detail by powder X-ray diffraction, thermal analysis, Fourier transform IR spectrometry, ^{1}H and ^{13}C NMR spectroscopy, UV spectroscopy, and single crystal X-ray diffraction.

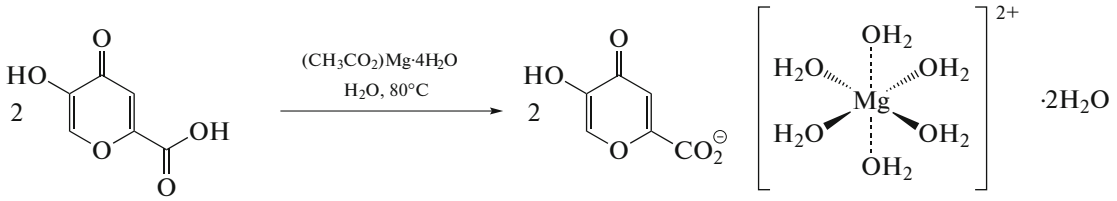

H_2L (**II**)

Scheme 1.

The phase identity was proved by powder X-ray diffraction. According to the experimental powder X-ray diffraction pattern, the sample of **I** had a crystalline structure and was characterized by a certain set of 2θ values, interplanar spacings d_{hkl}, and relative intensities I (%). The phase composition of the compound was determined by comparing the obtained experimental sets of 2θ and d_{hkl} values with the 2θ and d_{hkl} values of the reference X-ray diffraction patterns of single-phase compounds ($Mg(CH_3COO)_2\cdot 4H_2O$, comenic acid), which were recorded in advance.

Three X-ray diffraction patterns shown in Fig. 1 indicate the presence of phases of single compounds that belong to different crystallographic groups and the absence of amorphous impurities. The differences can be identified by few reflections that have the highest integral intensities. Indeed, d values (Å) were as follows: 7.03431, 6.92693, and 4.24540 for magnesium acetate; 3.13068, 4.76088, and 4.43165 for comenic acid; and 3.51591, 3.25920, and 3.11460 for the reaction product (magnesium comenate) (Fig. 1). A comparison of the interplanar spacings and relative intensities of the starting compounds and the synthesized coordination compound showed that the new compound differs significantly from the initial comenic acid. Hence, the resulting complex has an individual crystal lattice.

The thermal behavior and hydrate composition of the coordination compound were investigated by simultaneous thermal analysis. Figure 2 shows the thermal analysis curves (TG, DTG, and DSC), for magnesium comenate **I**. Thermolysis includes several stages. The DSC curve has an intense exotherm (–4.193 mW/mg), which attests to dehydration at a temperature below 205°C with a mass loss of 29.73% according to the TG curve, corresponding to elimination of eight water molecules. The high temperature of dehydration means that the water molecules occupy inner-sphere positions in the complex. Further temperature rise in the range of 205–304°C is accompanied by slight heat absorption (–1.122 mW/mg) with a mass loss of 11.83 and 3.94%, indicating intramolecular dehydration (elimination of one OH group) and decarboxylation of ligand molecules surrounding the Mg^{2+} cation. Presumably, intricate transformations associated with an intramolecular rearrangement into more favorable thermodynamic state take place in this case. In the temperature ranges of 304–400 and 400–575°C, the DSC curves show two pronounced exotherms (365.1°C,

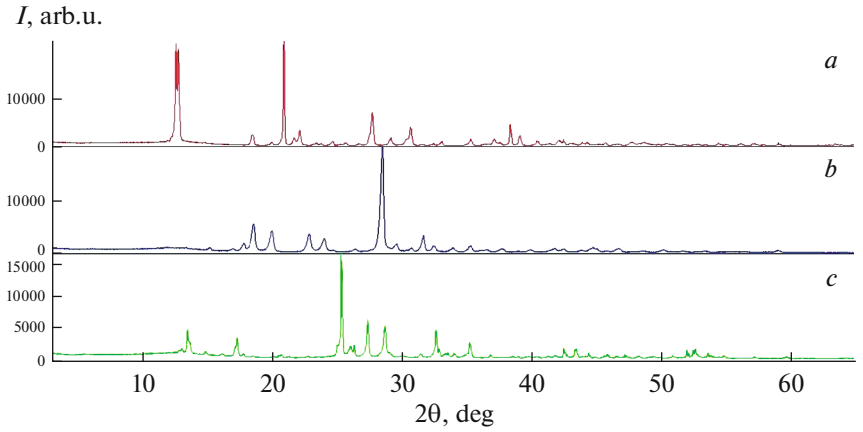

Fig. 1. Powder X-ray diffraction patterns of (*a*) magnesium acetate tetrahydrate; (*b*) comenic acid; (*c*) magnesium comenate **I**.

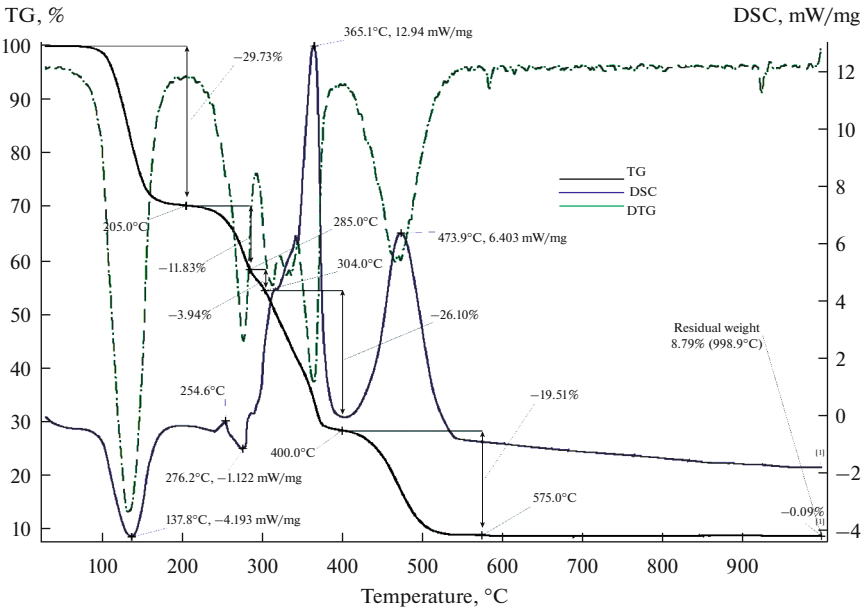

Fig. 2. TG, DTG, and DSC curves of complex **I**.

12.94 mW/mg and 473.9°C, 6.403 mW/mg). This is attributable to further thermolysis of the comenic acid remainders including two clearly defined steps accompanied by mass loss of 26.10% and then by 19.51%. The final thermolysis product is magnesium oxide, which is confirmed by the result of X-ray fluorescence elemental analysis of the incineration product. Table 1 summarizes the results obtained by physicochemical methods that were used to determine the general formula of magnesium comenate: $[Mg(HCom)_2(H_2O)_6]\cdot 2H_2O$.

The coordination mode of comenate anions ($HCom^-$) in the magnesium(II) complex was derived from IR spectroscopy data. The characteristic IR bands were assigned by comparing the IR spectra of the complex and H_2Com and by analysis of published data on β-hydroxy-γ-pyrones. In the IR spectrum (Table 2), the ν(O–H) band of H_2Com (3500 cm^{-1}) is shifted by 162 cm^{-1}, which attests to cleavage of the intramolecular hydrogen bonds in the initial ligand dimers (absorption bands at 3000–2400 cm^{-1}). The ν_{C-H} band of the γ-pyrone structure is broadened and overlaps with $\nu(O-H)(H_2O)$; this is in line with the results of thermal analysis, which shows the presence of numerous coordinated water molecules in the complex. The COOH stretching band in the IR spectrum of the complex is split into $\nu_{as}(COO^-)$ (1601 cm^{-1}) and $\nu_s(COO^-)$ (1352 cm^{-1}) bands. The difference is 249 cm^{-1}, which is much greater than 200 cm^{-1} and,

Table 1. Comparison of the results of physicochemical analysis obtained in determination of the molecular formula of magnesium comenate

Components of the complex	Found, wt %			Calculated, wt %
	thermogravimetry	X-ray fluorescence elemental analysis	complexometric titration	
Mg^{2+}	5.30	5.14	5.25	5.08
$HCom^-$	61.47	63.52		64.81
H_2O	29.73			30.11

Table 2. Characteristic frequencies (cm^{-1}) and their assignment in the IR spectra of comenic acid (H_2L) and magnesium comenate **I**

Compound	ν(O–H)	ν(C–H)	ν(O–H) (H_2O)	ν(C=O) (>C^4=O)	ν(C=O) (>COOH)	$\nu_{as}(COO^-)$	$\nu_s(COO^-)$	$\Delta\nu = \nu_{as}(COO^-) - \nu_s(COO^-)$	ν(C–O–C) (γ-pyrone)	ν(C–O)	ν(C–OH)	δ(C–OH)	ν(M–O)
H_2L	3338	3086	3000–2450	1726	1628				1219	1203	1144	1099	
I	3500	3093	3190–2975	1691		1601	1352	249	1271	1213	1157	1101	517

hence, each ligand in the complex is bound in the monodentate mode. The medium-intensity band at 517 cm^{-1} confirms the presence of the Mg–O bond.

The upfield shift of the H(3) proton signal in the ^1H NMR spectrum of magnesium comenate by 0.09 ppm in comparison with analogous signal in the comenic acid spectrum can be attributed to stronger electron-donating effect of COO^- in comparison with COOH. In the ^{13}C NMR spectrum, a number of signals shift downfield by (ppm) 1.15 for COOH, 2.12 for C(2), and for 0.96 C(3), which is indicative of deprotonation of the carboxyl group.

The UV spectrum of comenic acid (Table 3) exhibits a strong band at 199.5 nm (logε = 4.29) caused by the n–π* absorption of the chromophore carbonyl group as a part of carboxyl group. In the spectrum of complex **I**, this band is much weaker (Table 3) (logε 4.08) and transforms into a shoulder at the 222.4 nm band (logε 4.37), which corresponds to absorption of the =C–O–C= conjugated system of the γ-pyrone ring. The shift and the decrease in intensity of the band are due to the involvement of the COOH group into the complex formation.

Triclinic crystals suitable for X-ray diffraction were obtained by recrystallization of magnesium comenate **I** from water.

Complex **I** crystallizes with eight water molecules where six H_2O molecules form Mg^{2+} hydration shell, while the other two molecules bind the $[Mg(H_2O)_6]^{2+}$ aqua cation to ionized ligand molecules by intermolecular hydrogen bonds. The molecular structure of complex **I** is shown in Fig. 3; the dotted lines indicate the shortened contacts (Fig. 4) present in this structure. The packing of molecules in the crystal lattice is

Table 3. Characteristics of the absorption bands in the electronic spectrum of magnesium comenate **I**

λ_{max}, nm	Conjugated system	Transition	A, rel. u.	ε_{app}, L/mol cm*	$\log\varepsilon_{app}$
204.6	–COOH	$n \rightarrow \pi^*$	0.1205	19400	4.08
222.4	=C–O–C=	$n \rightarrow \pi^*$	0.2338	23380	4.37
246.8	>C=O	$n \rightarrow \pi^*$	0.0557	5570	3.75
285.2	–OH	$\pi \rightarrow \pi^*$	0.0588	5880	3.77

* ε_{app} is the apparent molar extinction coefficient.

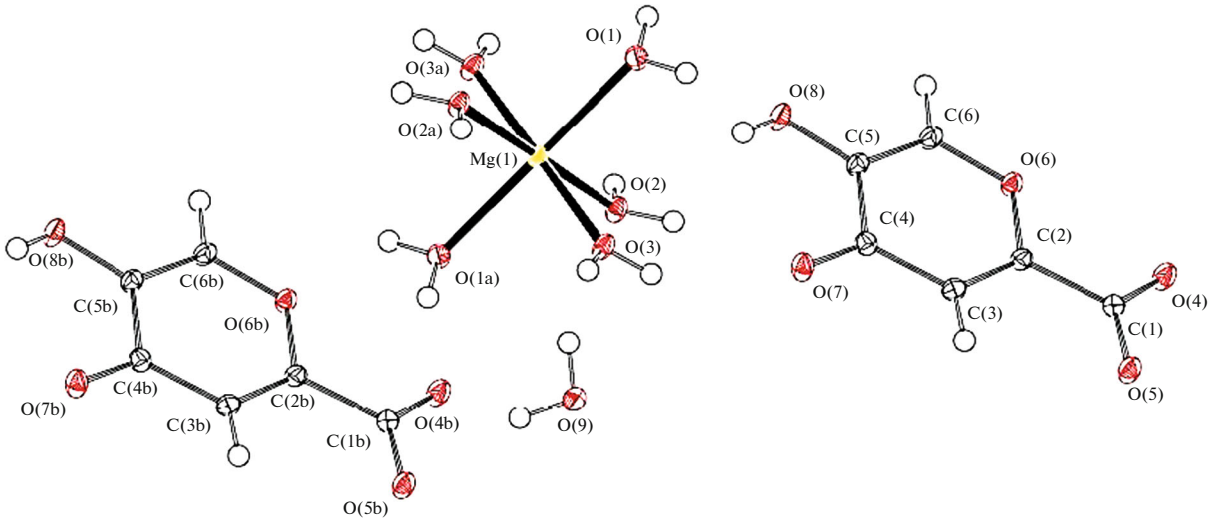

Fig. 3. General view of the molecule of magnesium complex with 5-hydroxy-4-oxo-4*H*-pyran-2-carboxylic acid in the crystal.

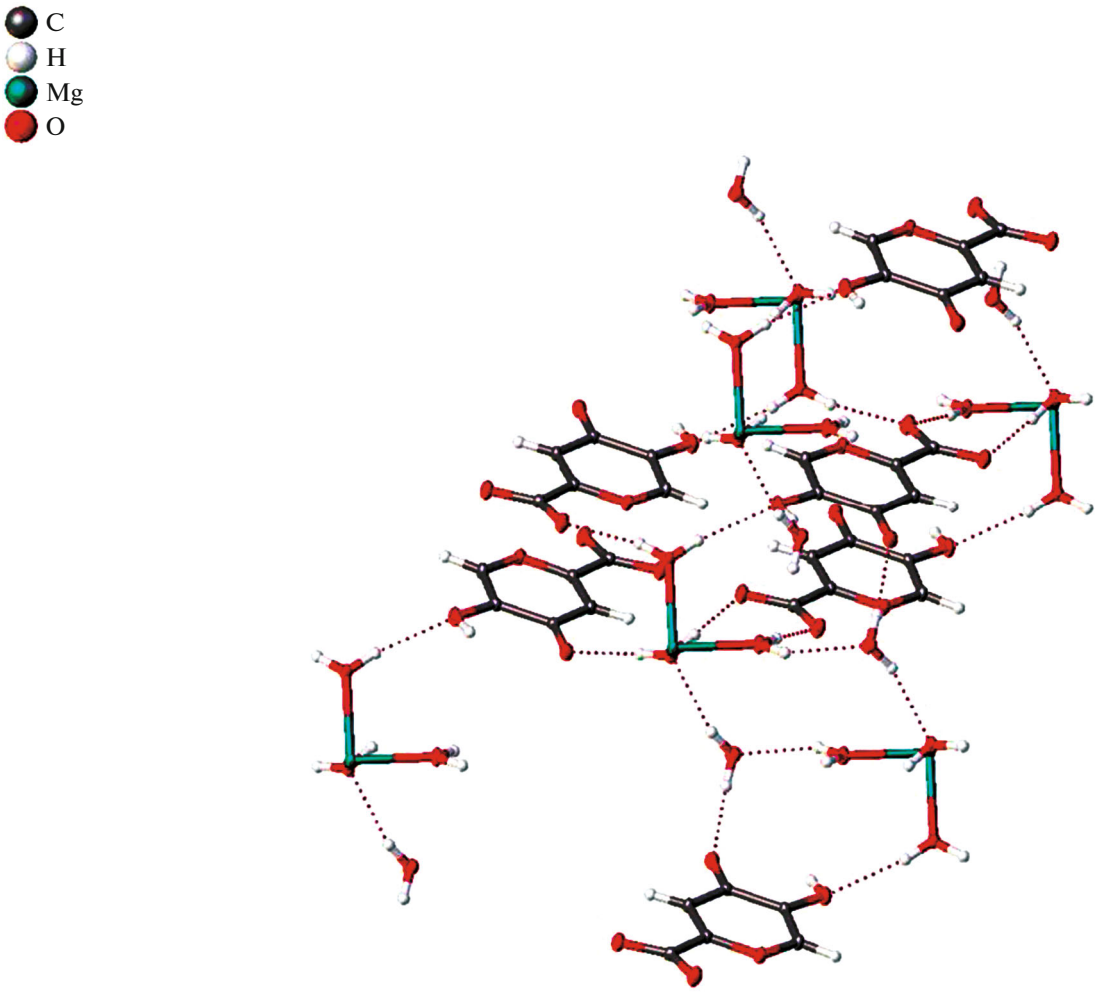

Fig. 4. Short intermolecular contacts in the crystal of magnesium comenate **I**.

Table 4. Crystallographic data, X-ray diffraction experiment and structure refinement details for magnesium comenate **I**

Parameter	Value
Molecular formula	$C_{12}H_{22}MgO_{18}$
M	478.60
Temperature, K	293(2)
System	Triclinic
Space group	$P\bar{1}$
a, Å	6.7265(2)
b, Å	7.0802(2)
c, Å	10.7367(4)
α, deg	103.337(3)
β, deg	96.095(2)
γ, deg	103.071(2)
V, Å^3	477.84(3)
Z	1
ρ(calcd.), g/cm^3	1.663
μ, mm^{-1}	1.711
F(000)	250.0
Crystal size, mm	0.417 × 0.324 × 0.307
Data collection range of 2θ, deg	8.584–152.2
Ranges of h, k, l	$-8 \le h \le 8$, $-8 \le k \le 8$, $-12 \le l \le 13$
Number of measured reflections	9635
Number of unique reflections (R_{int}, R_σ)	1990 (0.0180, 0.0104)
Data/constraints/parameters	1990/0/179
GOOF on F^2	1.107
R-factor ($I > 2\sigma(I)$)	$R_1 = 0.0248$, $wR_2 = 0.0655$
R-factor (all data)	$R_1 = 0.0251$, $wR_2 = 0.0657$
$\Delta\rho_{max}/\Delta\rho_{min}$, e Å^{-3}	0.38/–0.21

stabilized by a branched system of hydrogen bonds involving solvation water molecules and oxygen atoms of various functional groups of the ionized ligand molecules. The key crystallographic data and X-ray diffraction experiment details for this compound are summarized in Table 4. The most important bond lengths and bond angles within the coordination polyhedron are presented in Table 5. The Mg^{2+} ion occurs in the six-coordinate oxygen environment formed by the inner-sphere water molecules.

ACKNOWLEDGMENTS

This study was performed using the equipment of the Science and Education Center, Center for Collective Use "Diagnostics of Structure and Properties of Nanomaterials" (registration no. 3109) and equipment of the Center for

Table 5. Selected bond lengths and bond angles for $[Mg(HCom)_2(H_2O)_6]\cdot 2H_2O$ (**I**)

Bond	*d*, Å	Bond	*d*, Å
Mg(1)–O(2)[1]	2.0684(8)	O(8)–C(5)	1.3481(13)
Mg(1)–O(2)	2.0684(7)	O(7)–C(4)	1.2498(13)
Mg(1)–O(1)[1]	2.0841(8)	O(4)–C(1)	1.2508(13)
Mg(1)–O(1)	2.0841(8)	C(5)–C(4)	1.4512(14)
Mg(1)–O(3)	2.0400(8)	C(5)–C(6)	1.3519(15)
Mg(1)–O(3)[1]	2.0400(8)	C(4)–C(3)	1.4403(14)
O(6)–C(2)	1.3467(12)	C(2)–C(1)	1.5230(14)
O(6)–C(6)	1.3583(13)	C(2)–C(3)	1.3510(15)
O(5)–C(1)	1.2463(13)		
Angle	ω, deg	Angle	ω, deg
O(2)Mg(1)O(2)[1]	180.0	C(2)O(6)C(6)	118.94(8)
O(2)[1]Mg(1)O(1)[1]	90.83(3)	O(8)C(5)C(4)	120.80(9)
O(2)Mg(1)O(1)	90.83(3)	O(8)C(5)C(6)	119.27(9)
O(2[1])Mg(1)O(1)	89.17(3)	C(6)C(5)C(4)	119.90(10)
O(2)Mg(1)O(1)[1]	89.17(3)	O(7)C(4)C(5)	121.06(9)
O(1)[1]Mg(1)O(1)	180.00(3)	O(7)C(4)C(3)	124.32(9)
O(3)[1]Mg(1)O(2)[1]	86.85(3)	C(3)C(4)C(5)	114.60(9)
O(3)Mg(1)O(2)	86.85(3)	O(6)C(2)C(1)	112.80(9)
O(3)[1]Mg(1)O(2)	93.15(3)	O(6)C(2)C(3)	122.42(9)
O(3)Mg(1)O(2)[1]	93.15(3)	C(3)C(2)C(1)	124.77(9)
O(3)[1]Mg(1)O(1)[1]	90.32(3)	C(5)C(6)O(6)	122.96(9)
O(3)Mg(1)O(1)	90.32(3)	O(5)C(1)O(4)	127.81(10)
O(3)Mg(1)O(1)[1]	89.68(3)	O(5)C(1)C(2)	115.19(9)
O(3)[1]Mg(1)O(1)	89.68(3)	O(4)C(1)C(2)	116.99(9)
O(3)[1]Mg(1)O(3)	180.0	C(2)C(3)C(4)	121.06(10)

Symmetry codes: [1] $-x, 1-y, 2-z$.

Collective Use "Ecological and Analytical Center" (unique identifier RFMEFI59317X0008) of the Kuban State University.

FUNDING

This study was supported by the State Assignment of the Southern Scientific Center, Russian Academy of Sciences (AAAA-A19-119040390083-6) and by the Kuban Science Foundation in the framework of competition of the scientific innovative projects oriented towards commercialization (NIP-20.1/15).

CONFLICT OF INTEREST

The authors declare that they have no conflicts of interest.

REFERENCES

1. Cavalieri, L.F., *Chem. Rev.*, 1947, vol. 41, no. 3, p. 525. https://doi.org/10.1021/cr60130a004
2. Kandioller, W., Kurzwernhart, A., Hanif, M., et al., *J. Organomet. Chem.*, 2011, vol. 696, no. 5, p. 999.
3. Aida, K., *J. Agric. Chem. Soc. Jpn.*, 1955, vol. 19, no. 2, p. 97. https://doi.org/10.1080/03758397.1955.10857272
4. Shurygina, L.V., Zlishcheva, E.I., Kravtsov, A.A., et al., *Bull. Exp. Biol. Med.*, 2021, vol. 171, no. 3, p. 319. https://doi.org/10.47056/0365-9615-2021-171-3-319-322
5. Shurygina, L.V., Zlishcheva, E.I., Kravtsova, A.N., et al., *Bull. Exp. Biol. Med.*, 2017, vol. 163, no. 3, p. 344. https://doi.org/10.1007/s10517-017-3800-4
6. Shurygina, L.V., Zlishcheva, E.I., Kravtsov, A.A., et al., *Russ. J. Exp. Clin. Pharmacol.*, 2013, vol. 76, no. 8, p. 9. https://doi.org/10.30906/0869-2092-2013-76-8-9-12

7. Shurygin, A.Ya., Zlishcheva, L.I., Rasulov, Zh.G., and Ushakov, A.D., RF Patent 2026351, 1995.
8. Dik, O.E., Shelykh, T.N., Plakhova, V.B., et al., *Dokl. Biochem. Biophys.*, 2015, vol. 462, no. 1, p. 155. https://doi.org/10.7868/S086956521514025X
9. Rogachevskii, I.V., Plakhova, V.B., Domnin, I.N., et al., *Klin. Patofiziol.*, 2006, no. 1, p. 15.
10. Rogachevskii, I.V. and Plakhova, V.B., *Russ. J. Gen. Chem.*, 2006, vol. 76, no. 11, p. 1820. https://doi.org/10.1134/S1070363206110272
11. Fiorentini, D., Cappadone, C., Farruggia, G., et al., *Nutrients*, 2021, vol. 13, no. 4, p. 1136. https://doi.org/10.3390/nu13041136
12. Kirkland, A.E., Sarlo, G.L., and Holton, K.F., *Nutrients*, 2018, vol. 10, no. 6, p. 730. https://doi.org/10.3390/nu10060730
13. Shurygina, L.V., Zlishcheva, E.I., Kravtsov, A.A., et al., RF Patent 2528914, 2014.
14. Shurygina, L.V., Zlishcheva, E.I., Khablyuk, V.V., et al., *Bull. Exp. Biol. Med.*, 2015, vol. 159, no. 4, p. 466. https://doi.org/10.1007/s10517-015-2993-7
15. Shurygina, L.V., Zlishcheva, E.I., and Kravtsov, A.A., *Bull. Exp. Biol. Med.*, 2018, vol. 165, no. 4, p. 465. https://doi.org/10.1007/s10517-018-4195-6
16. Shurygin, A.Ya., Shurygina, L.V., and Lobova, N.N., RF Patent 2459623, 2012.
17. Shurygin, A.Ya., RF Patent 2287583, 2006.
18. Dolomanov, O.V., Bourhis, L.J., Gildea, R.J., et al., *J. Appl. Crystallogr.*, 2009, vol. 42, p. 339. https://doi.org/10.2138/am-2021-7785
19. Sheldrick, G.M., *Acta Crystallogr., Sect. A: Found. Adv.*, 2015, vol. 71, p. 3. https://doi.org/10.1107/S2053273314026370
20. Sheldrick, G.M., *Acta Crystallogr., Sect. C: Struct. Chem.*, 2015, vol. 71, p. 3. https://doi.org/10.1107/S2053229614024218

Translated by Z. Svitanko